

## Gel Filtration Chromatographic Study on the Micelle Formation of Triton X-100

Noriaki FUNASAKI,\* Sakae HADA, and Saburo NEYA  
Kyoto Pharmaceutical University, Yamashina-ku, Kyoto 607  
(Received November 17, 1988)

The aggregation properties of Triton X-100 are investigated by frontal gel (Sephadex G-200) filtration chromatography (GFC) at 25 °C and considered in the framework of the monomer- $m$ -mer equilibrium on the basis of both asymptotic and plate theories. The analysis of GFC data by asymptotic theory yields an equilibrium constant of  $K=1.3 \times 10^{68}$  ( $\text{mmol dm}^{-3}$ )<sup>-138</sup> and a micellar elution volume of  $V_m=15.30$  cm<sup>3</sup>. By using this  $V_m$  value, we calculate a micellar hydrodynamic radius of 4.6 nm and the monomer concentration  $C_1$  for Triton X-100. Values of  $\text{cmc}=0.30$  mmol dm<sup>-3</sup> (UV at 245 nm) and 0.31 mmol dm<sup>-3</sup> (UV at 265 nm and GFC) are determined and are very close to the cmc value theoretically calculated by using Phillips' definition of the cmc. The  $C_1$  value above the cmc is larger than these cmc values by about 0.06 mmol dm<sup>-3</sup>. The derivative elution pattern at the trailing boundary exhibits two maxima and a minimum ( $V_{\min}$ ), and indicates the formation of small micelles near the cmc. The concentration at  $V_{\min}$  on the elution curve,  $C_{\min}$ , is close to the cmc, as we have already predicted by both asymptotic and plate theories. The present work demonstrates the utility of these theories for analyzing the GFC pattern of self-associating systems and will serve to understand the actions of Triton X-100 on membrane bound proteins and on lipid bilayers.

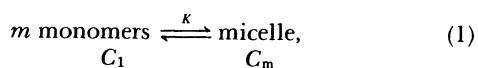
Triton X-100 is a commercial, polydisperse preparation of polyethylene glycol mono[ $p$ -(1,1,3,3-tetra-methylbutyl)phenyl] ethers, containing an average of 9.6 oxyethylene units per molecule. This surfactant is very frequently used in the isolation and study of membrane bound proteins and water insoluble lipids. Furthermore, this interaction of membrane proteins with Triton X-100 monomers and micelles can provide information on the mechanism whereby they are attached within membranes.<sup>1,2)</sup> Micelle formation of Triton X-100 in aqueous solution has been studied by light scattering,<sup>3-5)</sup> viscosity,<sup>5,6)</sup> ultracentrifugation,<sup>5-8)</sup> fluorescence,<sup>8)</sup> gel filtration chromatography (GFC),<sup>5,9)</sup> and small-angle X-ray scattering measurements.<sup>5)</sup>

For the quantitative investigation of self-associating systems by GFC, the large sample size (frontal) method is superior to the small sample size (zonal) method.<sup>10-14)</sup> Recently, we developed a plate theory based on mass action model for micelle formation,<sup>13,14)</sup> but this theory has rarely been used for analysis of GFC data on surfactants. Furthermore, asymptotic theory provides analytical solutions for GFC patterns, but most of them have not yet been used for surfactants.<sup>10-14)</sup>

In this work, we report the frontal GFC elution curve and its derivative for Triton X-100 as a function of concentration at 25 °C. These data are analyzed with the above-mentioned theories. The aggregation properties obtained of Triton X-100 are compared with those by other workers.

### Theoretical Basis

For the sake of simplicity, we regarded the micelle formation of a nonionic surfactant as the following equilibrium:



where  $C_1$  and  $C_m$  denote the molarities of monomer and  $m$ -mer of the surfactant on a monomer basis. The equilibrium constant  $K$  of this reaction may be written as

$$K=C_m/C_1^m. \quad (2)$$

The total molarity  $C_0$  of surfactant can be written as

$$C_0=C_1+C_m=C_1+KC_1^m. \quad (3)$$

When a large volume of a sample with the concentration  $C_0$  is charged in a column, a plateau region with the same concentration appears on the elution curve, e.g., as shown in Fig. 1a. Approximately, we may assume that the equivalent sharp boundary for the solute zone leading or trailing boundary is the first moment (centroid) of the elution profile and satisfies the relationships:<sup>10)</sup>

$$V_c=\int_0^{C_0} VdC/C_0 \quad (\text{leading boundary}) \quad (4)$$

and

$$V'_c=\int_0^{C_0} VdC/C_0+S \quad (\text{trailing boundary}), \quad (5)$$

where  $S$  is the charged volume of the sample. For these determinations the volume coordinate  $V$  is assigned a zero value when the leading boundary of the charged sample enters the column bed. According to this approximation (called asymptotic theory), the elution curve for a nonassociable solute is expected as a rectangle of  $C_0$  in height and of  $S$  in width.

Above the cmc (for the case of  $m \geq 3$ )<sup>10,13)</sup> the second "plateau region" generally appears at the trailing boundary. This region is clearly shown in its derivative, e.g., as shown in Fig. 1b. According to the asymptotic theory we can expect the derivative pattern shown by the dot-dash line and the following equations:<sup>10,13,14)</sup>

$$m=(3V_{\min}-V_1-2V_m)/(3V_{\min}-2V_1-V_m), \quad (6)$$

$$K=(m-2)[2(m^2-1)]^{m-1}/[m(2m-1)]^m/(C_{\min})^{m-1}, \quad (7)$$

$$V_c = C_1 V_1 / C_0 + C_m V_m / C_0, \quad (8)$$

and

$$V_c = (V_1 - V_m)^{(m-1)/m} C_0^{(1-m)/m} (V_1 - V_c)^{1/m} / K^{1/m} + V_m. \quad (9)$$

Here  $V_1$  and  $V_m$  denote the centroid elution volumes of the monomer and the micelle and  $C_{\min}$  may be taken as the concentration corresponding to the minimum  $V_{\min}$  on the derivative curve (Fig. 1). Both  $V_{\min}$  and  $C_{\min}$  are expected to be independent of  $C_0$  from Eqs. 6 and 7.

According to plate theory, a gel column may be assumed to be composed of  $n$  plates and each plate consists of the mobile and stationary phases. The total volume of the mobile phase equals to the void volume of the column. The partition ratio,  $P$ , of a solute between these phases may be written as

$$P = (V_c - V_0) / V_0, \quad (10)$$

where  $V_c$  is the elution volume of the solute and  $V_0$  the void volume. Assuming appropriate values for  $V_0$ ,  $n$ ,  $V_1$ ,  $V_m$ ,  $K$ ,  $m$ , and  $C_0$ , we can simulate the theoretical elution curve and its first-derivative curve. The plate theory predicts more realistic elution and derivative patterns than the asymptotic theory. The computer simulation procedure of the plate theory has been reported in detail elsewhere.<sup>14)</sup>

In the both theories, micelle formation and partition equilibrium of surfactant are assumed to be instantaneously established.<sup>14)</sup>

### Experimental

**Materials.** Triton X-100 was purchased from Tokyo Kasei Organic Chemicals. Sephadex G-200 was obtained from Pharmacia Fine Chemicals and used as suggested by the manufacturer.<sup>15)</sup> Four proteins whose hydrodynamic radii  $R_h$  (nm) are known<sup>15,16)</sup> were used as standards for the determination of  $R_h$  of the Triton X-100 micelle. From Sigma are whale myoglobin type II ( $R_h=1.9$ ), bovine serum albumin ( $R_h=3.5$ ), yeast alcohol dehydrogenase ( $R_h=4.6$ ), and thyroglobulin ( $R_h=8.5$ ). The ion-exchanged water was twice distilled and degassed before use.

**Methods.** A gel column of an inner diameter of 1 cm and a total gel volume of  $V_t=26.94 \text{ cm}^3$  was jacketed to maintain a constant temperature at  $25 \pm 0.2^\circ \text{C}$ . A sample or eluent was flown into the column at a constant flow rate of about  $8 \text{ cm}^3 \text{ h}^{-1}$  by using a mini-pump. The concentration of Triton X-100 in eluate was continuously monitored with a Shimadzu SPD-2A spectrophotometric detector and recorded with a Shimadzu Chromatopac C-R1B data processor. A wavelength of 265 nm or 245 nm was used for absorbance measurements. The absorbance was converted to concentration by using the absorbances of several Triton X-100 solutions at known concentrations.

Computer simulation was carried out with an NEC PC-9801 VX personal computer.

### Results and Discussion

**Frontal GFC Patterns of Triton X-100.** The elution curve, like Fig. 1a, was determined at 10 concentrations ( $C_0=0.203\text{--}10.048 \text{ mmol dm}^{-3}$ ). From the

leading and trailing boundaries, we can determine the centroid volumes,  $V_c$  and  $V_c'$ . Since these values were in a agreement with each other within experimental errors, we used the average of them hereafter. As Fig. 2 shows,  $V_c$  rapidly decreased with an increase of  $C_0$  above the cmc (Table 1). These  $V_c$  values were plotted against  $1/C_0$  in Fig. 3. From the intersection of two straight lines drawn above and below the cmc, we determined a cmc value of  $0.31 \text{ mmol dm}^{-3}$ . This value is very close to the cmc values obtained from the absorbance- $C_0$  plots at 265 nm and 245 nm, as well as

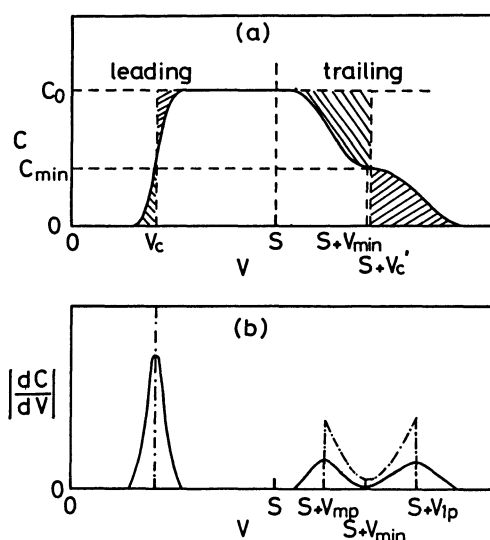


Fig. 1. Schematic elution curve (a) and its derivative (b) for a micellar system and definitions of characteristic parameters. The shaded areas around  $V_c$  and  $V_c'$  are related to Eqs. 4 and 5. The dot-dash line shows the derivative curve predicted by asymptotic theory and the solid lines show the observed results and those predicted by plate theory.

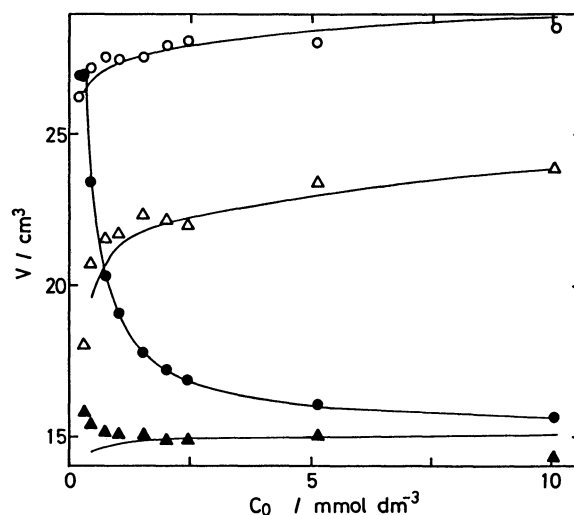


Fig. 2. Characteristic elution volume parameters as a function of total concentration for Triton X-100:  $\circ$ ;  $V_{1p}$ ,  $\Delta$ ;  $V_{\min}$ ,  $\bullet$ ;  $V_c$ ,  $\blacktriangle$ ;  $V_{\max}$ . The solid lines show the computer-simulated values.

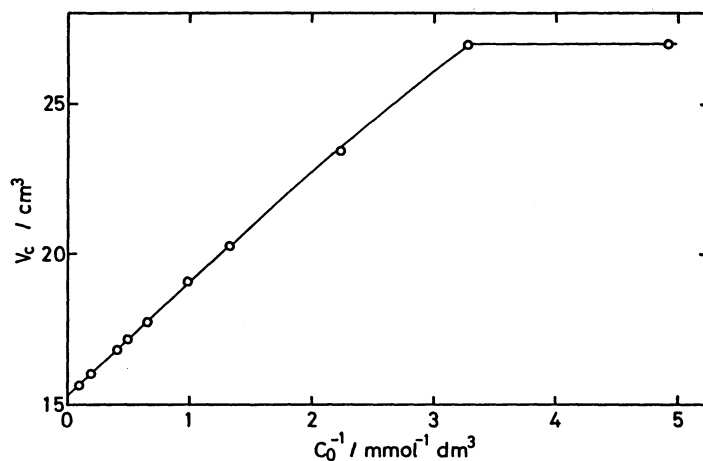


Fig. 3. Centroid volumes as a function of reciprocal concentration for Triton X-100. The solid line shows the computer-simulated values.

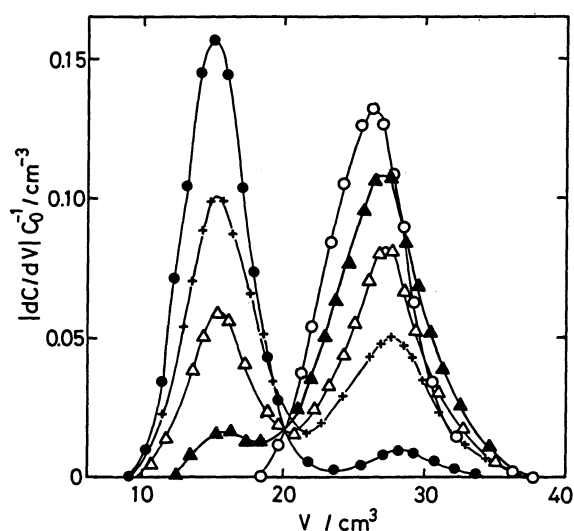


Fig. 4. Reduced derivative elution curves for Triton X-100 at five concentrations (mmol dm<sup>-3</sup>): ○; 0.203, ▲; 0.305, △; 0.448, +; 0.753, ●; 5.123.

to the literature value.<sup>17)</sup>

Figure 4 shows the reduced derivative profiles for the trailing boundary at five concentrations, where the volume coordinate  $V$  is assigned a zero value when eluent enters the column bed. At  $C_0=0.305$  mmol dm<sup>-3</sup> a small peak of the micelle appears together with a large peak of the monomer. From the elution and derivative profiles we can determine values of  $V_{1p}$ ,  $V_{mp}$ ,  $V_{min}$ , and  $C_{min}$ . In Fig. 2 are shown  $V_{1p}$ ,  $V_{mp}$ , and  $V_{min}$  as a function of  $C_0$ . Values of  $C_{min}$  are shown in Fig. 5.

Triton X-100 is not a pure substance, but a lot of data have been analyzed with the assumption that it was a pure surfactant.<sup>3-8)</sup> A number of  $m$  values near 25 °C have been reported;  $m=139$  (room temperature)<sup>3)</sup> and 135 (25 °C)<sup>4)</sup> by light scattering,  $m=134$  (20 °C),<sup>6)</sup> 100 (25 °C),<sup>7)</sup> and 125 (25 °C, 10 mmol dm<sup>-3</sup> phosphate buffer)<sup>8)</sup> by ultracentrifugation,  $m=121$  (25 °C, 10

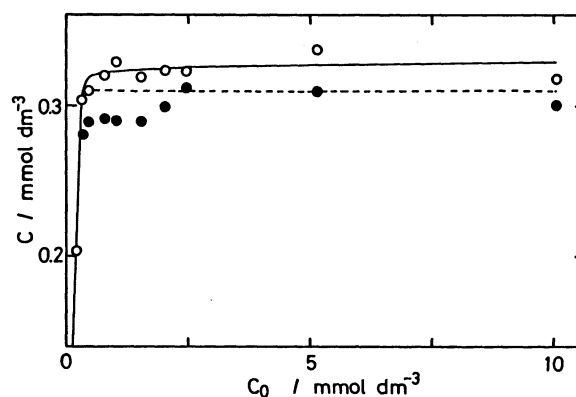


Fig. 5. Values of monomer concentration  $C_1$  (○) and  $C_{min}$  (●) as a function of total concentration for Triton X-100. The solid line was calculated from Eq. 3 and the dashed line was computer-simulated for  $C_{min}$ .

mmol dm<sup>-3</sup> phosphate buffer) by fluorescence titration,<sup>8)</sup> and  $m=147$  (20 °C) and 231 (30 °C) by small-angle X-ray scattering.<sup>5)</sup> For the purpose of analysis of our GFC data, we used a value of  $m=139$ . When  $m$  is a large value like this, analyzed results little change with variation in  $m$ .

Figure 6 shows the plot according to Eq. 9 by employing  $m=139$  and  $V_1=27.00$  cm<sup>3</sup>. This  $V_1$  value was taken from  $V_c$  at  $C_0=0.203$  mmol dm<sup>-3</sup>, the lowest concentration used herein. From this plot we can estimate values of  $K=1.3 \times 10^{68}$  (mmol dm<sup>-3</sup>)<sup>-138</sup> and  $V_m=15.30$  cm<sup>3</sup>. By using the linear relationship between  $\{(-\log[(V_c-V_0)/(V_1-V_0)])^{1/2}$  and  $R_h$  for the proteins described in the Experimental section, we estimated a value of  $R_h=4.6$  nm for the Triton X-100 micelle from this  $V_m$  value. This  $R_h$  value is consistent with the literature values shown in Table 1.<sup>5,6,9)</sup>

From Eq. 8 we can estimate the monomer concentration  $C_1$  by using the above values of  $V_1$  and  $V_m$ . The  $C_1$  values thus obtained are shown in Fig. 5.

Table 1. Values of Cmc and  $R_h$  for Triton X-100 Micelles at 25 °C

Method	Cmc	$R_h(\text{temp})$	Reference
	mmol dm <sup>-3</sup>	nm	
GFC	0.309		This work
UV	0.30(245nm)		This work
UV	0.31(265nm)		This work
Calcd <sup>a)</sup>	0.309		This work
Dialysis	0.3		17
GFC		4.6	This work
GFC		4.1(20 °C)	9
GFC		4.0(20 °C)	5
GFC		5.5(30 °C)	5
DLS <sup>b)</sup>		4.2(20 °C)	5
DLS <sup>b)</sup>		5.6(30 °C)	5
SV <sup>c)</sup>		4.8(20 °C)	6

a) Calculated from Eq. 11. b) Dynamic light scattering. c) Sedimentation velocity.

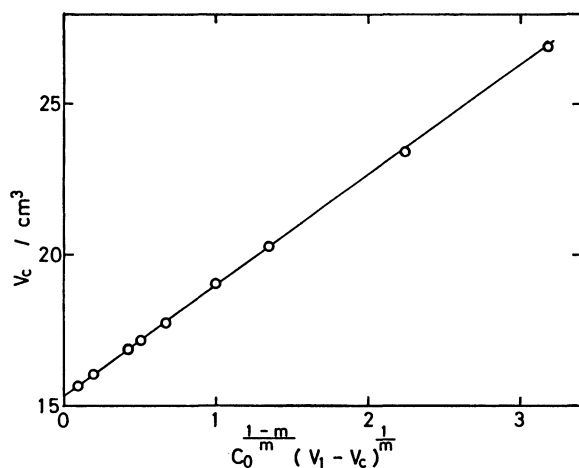


Fig. 6. Centroid volumes plotted according to Eq. 9. The straight line was fitted to the seven high-concentration data by the least-squares method.

The monomer concentration above the cmc is usually assumed to be equal to cmc. As Fig. 5 shows,  $C_1$  is slightly larger than cmc. This is an important result when one considers various actions of Triton X-100.

**Comparison between Theory and Experiment.** By using the estimated values of  $V_1$ ,  $V_m$ , and  $m$ , we can calculate a value of  $V_{\min}=23.13$  cm<sup>3</sup> from Eq. 6, regardless of  $C_0$ . This value is close to the observed values of  $V_{\min}$  shown in Fig. 2, but Eq. 6 cannot explain the observed increase of  $V_{\min}$  with increasing  $C_0$ . By using the estimated values of  $K$  and  $m$ , we can calculate a value  $C_{\min}=0.309$  mmol dm<sup>-3</sup> from Eq. 7, regardless of  $C_0$ . This value is similar to the observed  $C_{\min}$  values shown in Fig. 5, and practically the same to the cmc values shown in Table 1. Recently, by using Phillips' definition of the cmc,<sup>18)</sup> we could derive the equation:<sup>14)</sup>

$$\text{cmc} = [Km(2m-1)/(m-2)]^{1/(1-m)}. \quad (11)$$

When  $m$  is large enough, we can obtain from Eqs. 7 and 11

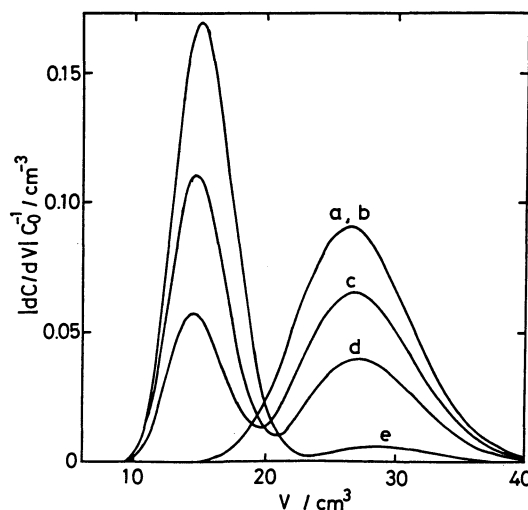


Fig. 7. Computer-simulated derivative patterns at five concentrations (mmol dm<sup>-3</sup>): a; 0.203, b; 0.305, c; 0.448, d; 0.753, e; 5.123.

$$C_{\min} = \text{cmc} = (2Km)^{1/(1-m)}. \quad (12)$$

Substitution of the estimated values of  $m$  and  $K$  yields a value of  $C_{\min} = \text{cmc} = 0.309$  mmol dm<sup>-3</sup>. This result explains the experimental observation that  $C_{\min}$  is close to cmc.

Based on the plate theory, we can computer-simulate the elution curve and its derivative by assuming appropriate values for  $V_0$ ,  $n$ ,  $V_1$ ,  $V_m$ ,  $K$ ,  $m$ , and  $C_0$ . For  $V_1$ ,  $V_m$ ,  $K$ , and  $m$  we used the values estimated above, and regarded  $V_0$  and  $n$  as fitting parameters; we used  $V_0 = 5.0$  cm<sup>3</sup> and  $n = 30$ .

The solid lines for  $V_c$  shown in Figs. 2 and 3 were computed by the plate theory and are very close to the observed values, as expected; for many  $m$  values we have theoretically shown that the plate theory and Eq. 8 predict the same value for  $V_c$ .<sup>13,14)</sup> Figure 7 shows the derivative elution profiles at the five concentrations, corresponding to Fig. 4. These figures show similar results, except the results at  $C_0 = 0.305$  mmol dm<sup>-3</sup>. At this concentration the micellar peak experimentally observed do not appear on the theoretical curve. This discrepancy will be considered below. As Fig. 2 shows, the plate theory explains the increase of  $V_{1p}$  and  $V_{\min}$  with increasing  $C_0$ , whereas it predicts a minor increase of  $V_{mp}$  with increasing  $C_0$ . As Fig. 5 shows, the computed  $C_{\min}$  values (dashed line) decreased only slightly with increasing  $C_0$  and are very close to the cmc values shown in Table 1.

**Aggregation Properties of Triton X-100.** Triton X-100 is an important surfactant for the investigation of biological membranes.<sup>1,2)</sup> To consider the action of Triton X-100 on biological membranes, we need to estimate the concentrations of the monomer and the micelle. In most cases the monomer concentration  $C_1$  is taken as the cmc. From the analysis of our GFC data, we determined  $C_1$  as a function of  $C_0$ . As Fig. 5 shows,  $C_1$  is larger than the cmc by about 0.06 mmol

dm<sup>-3</sup>. From Eq. 12 we can estimate the  $K$  value by using the cmc and  $m$  values and subsequently we can estimate the  $C_1$  value from Eq. 3 by using these  $m$  and  $K$  values. The estimated  $C_1$  value may be used, when no observed  $C_1$  value is available. Another reason why we chose this surfactant is that its concentration can be very accurately determined by ultraviolet spectroscopy (UV). Most surfactants do not absorb ultraviolet or visible light. Therefore the refractive index (RI) measurement is usually used for monitoring their concentrations.<sup>12)</sup> Generally speaking, UV is a more accurate method than the RI method, since the UV absorbance is less temperature-dependent than RI. An accurate concentration determination is essential for obtaining the derivative elution curve.

According to Makino et al.<sup>17)</sup> typical samples of Triton X-100 consist of 93% polyethylene glycol mono(octylphenyl) ether and 7% of polyethylene glycol bis(octylphenyl) ether. Most of it is *p*-substituted, but about 10% of the mono-octyl ether and the second alkyl group of the dioctyl ether are *o*-substituted. The presence of these impurities must be taken into consideration.

Zonal GFC,<sup>5,9)</sup> viscosity,<sup>5,6)</sup> and ultracentrifugation<sup>5,8)</sup> measurements have all suggested that the size of Triton X-100 micelles little changes with variation of  $C_0$  around 25 °C (it should be noted that these measurements were not carried out at low concentrations). This result is consistent with the data of Tanford et al.<sup>19)</sup> They showed that micelles of dodecyl ethers possessing eight or more oxyethylene units do not grow with increasing  $C_0$  at 25 °C.

Assuming only the micelle with an aggregation number of 139, we have applied the asymptotic and plate theories to our frontal GFC data. Taking into consideration inaccuracies of both these data and theories, agreement between theory and experiment in Figs. 2–5 and 7 is generally good except at low concentrations near the cmc. As Fig. 4 shows, a micellar peak appears at  $C_0 = 0.305$  mmol dm<sup>-3</sup>. At the same concentration, however, no micellar peak is observed on the computer-simulated curve (Fig. 7). Furthermore, as Fig. 2 shows, the observed  $V_{mp}$  values at low concentrations are larger than those predicted by the plate theory. These results indicate the presence of small micelles at low concentrations and are consistent with light scattering data at low concentrations.<sup>3)</sup> The formation of the small micelles may result in negative deviations of the observed  $V_1$  and  $C_{min}$  values from the theoretical values at low concentrations (Fig. 5). These small micelles will contain the dioctyl ether preferentially, since the dioctyl ether is expected to be more surface-active than the mono-octyl ether.

In this work, the micelle formation of Triton X-100 was analyzed in terms of the monomer- $m$ -mer equilibrium, but we showed that smaller micelles are formed near the cmc. When attempting to take into

consideration the concentration dependence of  $m$ , we encounter the difficulty that Triton X-100 contains the above-mentioned impurities. Therefore we must consider the concentration dependences of  $m$  and the micellar composition for this surfactant. Prior to overcoming this difficulty, we must understand the concentration dependence of  $m$ . This may be possible for pure surfactants.<sup>20)</sup> Furthermore, from the theoretical view-point, the concentration of the micelle should be expressed as the "true" molarity, viz.,  $C_m/m$ , and then the equilibrium constant should be denoted as  $K/m$ .

### Conclusion

The monomer concentration  $C_1$  for Triton X-100 was determined as a function of total concentration from the concentration dependence of the centroid volume by using the asymptotic theory. This  $C_1$  value was close to that expected from the monomer- $m$ -mer equilibrium with values of  $m = 139$  and  $K = 1.3 \times 10^{68}$  (mmol dm<sup>-3</sup>)<sup>-138</sup>. Observed values of cmc = 0.30 mmol dm<sup>-3</sup> (UV) and 0.31 mmol dm<sup>-3</sup> (UV and GFC) were smaller than the  $C_1$  value by about 0.06 mmol dm<sup>-3</sup>. The above-mentioned  $K$  value was determined from the concentration dependence of the centroid volume. The hydrodynamic radius of the Triton X-100 micelle was determined to be 4.6 nm from the elution volume  $V_m$  of the micelle. The derivative elution pattern showed the formation of small micelles near the cmc. The plate theory and asymptotic theory were useful for analyzing the elution curve and its derivative for Triton X-100. These results will serve to understand the mechanism of actions of Triton X-100 on biological membranes.

Thanks are due to Professor J. Paiement, Laval University, Canada, for helpful discussion and to Ms. A. Ohtani and Mr. M. Tanigawa for technical assistance.

### References

- 1) A. Helenius and K. Simons, *Biochim. Biophys. Acta*, **415**, 29 (1975).
- 2) C. Tanford and J. A. Reynolds, *Biochim. Biophys. Acta*, **457**, 133 (1976).
- 3) L. M. Kushner and W. D. Hubbard, *J. Phys. Chem.*, **58**, 1163 (1954).
- 4) A. M. Mankowich, *Ind. Eng. Chem.*, **47**, 2175 (1955).
- 5) H. H. Paradies, *J. Phys. Chem.*, **84**, 599 (1980).
- 6) S. Yedgar, Y. Barenholz, and V. G. Cooper, *Biochim. Biophys. Acta*, **363**, 98 (1974).
- 7) C. W. Diggins, R. J. Bolen, and H. N. Dunning, *J. Phys. Chem.*, **64**, 1175 (1960).
- 8) C. J. Biaselle and D. B. Millar, *Biophys. Chem.*, **3**, 355 (1975).
- 9) R. J. Robson and E. A. Dennis, *Biochim. Biophys. Acta*, **573**, 489 (1979).
- 10) G. K. Ackers, *Adv. Protein Chem.*, **24**, 343 (1970).
- 11) T. Sasaki, *Yukagaku*, **16**, 49 (1967).

- 12) N. Funasaki, S. Hada, and S. Neya, *J. Phys. Chem.*, **92**, 3488 (1988).
  - 13) N. Funasaki, S. Hada, and S. Neya, *Bull. Chem. Soc. Jpn.*, **61**, 2961 (1988).
  - 14) N. Funasaki, S. Hada, and S. Neya, *Bull. Chem. Soc. Jpn.*, **62**, 380 (1989).
  - 15) Pharmacia technical bulletin "Gel Filtration. Theory and Practice."
  - 16) L. M. Siegel and K. J. Monty, *Biochim. Biophys. Acta*, **112**, 346 (1966).
  - 17) S. Makino, J. A. Reynolds, and C. Tanford, *J. Biol. Chem.*, **248**, 4926 (1973).
  - 18) J. N. Phillips, *Trans. Faraday Soc.*, **51**, 561 (1951).
  - 19) C. Tanford, Y. Nozaki, and M. F. Rohde, *J. Phys. Chem.*, **81**, 1550 (1977).
  - 20) N. Funasaki, S. Hada, and S. Neya, manuscript in preparation.
-